*Geochimica et Cosmochimica Acta* Vol. 57, pp. 2101–2110


0016-7037/93/$6.00 + .00

# Thermoluminescence and compositional zoning in the mesostasis of a Semarkona group A1 chondrule and new insights into the chondrule-forming process

SATOSHI MATSUNAMI,[1,*] KIYOTAKA NINAGAWA,[2,†] SATORU NISHIMURA,[2] NORIKO KUBONO,[2]
ISAO YAMAMOTO,[3] MASAKI KOHATA,[3] TOMONORI WADA,[4] YOSHIHIKO YAMASHITA,[4]
JIE LU,[5] DEREK W. G. SEARS,[5] and HIROSHI NISHIMURA[1]

[1]Department of Geosciences, Naruto University of Education, Takashima, Naruto 772, Japan
[2]Department of Applied Physics, Okayama University of Science, Ridai-cho 1-1, Okayama 700, Japan
[3]Department of Electronic Engineering, Okayama University of Science, Ridai-cho 1-1, Okayama 700, Japan
[4]Department of Physics, Okayama University, Tsushimanaka 3-1-1, Okayama 700, Japan
[5]Cosmochemistry group, Department of Chemistry and Biochemistry, University of Arkansas, Fayetteville, AR 72701, USA

(*Received February* 13, 1992; *accepted in revised form October* 28, 1992)

**Abstract**—A large, group A1, porphyritic olivine chondrule in the Semarkona (LL3.0) chondrite with induced thermoluminescence (TL) and compositional zoning in its mesostasis has been discovered. The chondrule has Ca-rich and Fe-poor olivine (CaO, 0.36–0.40 wt%, $Fa_{0.3-0.5}$) and its mesostasis is highly anorthite-normative (~52.5 wt%). The chondrule shows an intense induced TL peak at ~300°C with a half-width of ~180°C. The induced TL in the 40–440°C range increases monotonically by a factor of ~6 from center to rim, while $SiO_2$, $Na_2O$, and MnO increase by factors of ~1.1, ~3.6, and ~6, respectively. The spectrum of the induced TL over the 200–350°C range (i.e., a dominant peak at ~570 nm with a half-width of about 100 nm) and the Mn-TL correlation suggest Mn-activated plagioclase is an important constituent of the refractory mesostases in group A1 chondrules.

The zoning may reflect fractional crystallization, Soret diffusion, transport of volatiles into the chondrule by aqueous alteration, a zoned precursor, reduction of precursor dust aggregate, or recondensation of volatiles lost during chondrule formation. The first four possibilities seem unlikely explanations for the zoning of the mesostasis, but both reduction of precursor dust aggregate and recondensation of volatiles seem to have played significant roles to the formation of the zoning. Reducing conditions at high temperatures are suggested to have prevailed during the formation of group A1 chondrules.

## INTRODUCTION

THE TL SENSITIVITY OF ORDINARY chondrites increases by 5 orders of magnitude during metamorphism due to the formation of feldspar (GUIMON et al., 1986; SEARS, 1988). Thus, TL sensitivity is a precise indicator of low-grade metamorphism of type 3 ordinary chondrites and shows correlations with many metamorphism-sensitive properties (SEARS et al., 1980, 1991; SCOTT, 1984). These earlier studies were made entirely on bulk samples and physically separated chondrules, but it seems very likely that detailed study of the relationship between TL and petrography will reveal new details concerning the origin and metamorphic history of primitive solar system material. Certainly, the closely related cathodoluminescence (CL) and petrography have provided several new insights (STEELE, 1986; DEHART and SEARS, 1986; SEARS et al., 1989; DEHART et al., 1992a). Based on CL and compositional data, SEARS et al. (1992) have recently identified two series involving eight groups of chondrules; the A1 to A5 series in which chondrules with plagioclase-normative mesostases and Ca-rich and Fe-poor olivine underwent major compositional changes into chondrules with oligoclase-normative mesostasis and Ca-poor, Fe-rich olivines with increasing metamorphism and the B1 to A5 series in which the same end product is derived from chondrules with silica-normative mesostasis but Ca-poor, Fe-rich olivines. However, while CL has proved very useful in these studies, it does not provide information on TL peak temperature or width which provide independent information on the thermal history of the samples (SEARS, 1988).

We recently began studies of the induced TL petrography of primitive type 3 chondrites using a system involving image intensification and solid state detectors coupled to video-recording equipment (WALTON and DEBENHAM, 1980; IMAEDA et al., 1985; NINAGAWA et al., 1990). Previous works with this system have shown (1) that silica phase in ALHA77214 (L3.4) is a common source of TL, as well as the widely assumed feldspathic phases (MATSUNAMI et al., 1992); (2) that there is a relationship between TL peak temperature and width and composition for chondrule mesostasis (NINAGAWA et al., 1991); and (3) that the TL of some chondrules with anorthite-normative mesostases in Semarkona (LL3.0) and Bishunpur (LL3.1) is produced at wavelengths > 480 nm (NINAGAWA et al., 1992). In the present paper, we concentrate on a large (~800 μm) group A1 chondrule in Semarkona (LL3.0) which contains induced TL and compositional zoning in the mesostasis. We suggest that this chondrule provides new insights into processes accompanying the formation of this significant type of chondrule.

## EXPERIMENTAL

A 50.47 mg chip of the Semarkona (LL3.0) chondrite (USNM 1805) was cut into three slices by a wire saw, which were fixed onto metallic plates with epoxy resin and ground to 1 mm thickness with

* *Temporary address:* Max-Planck-Institut für Kernphysik, Postfach 103980, D-6900 Heidelberg 1, Germany.
† Author to whom correspondence should be addressed.

alumina and polished with diamond paste. The samples were then given a 13.2 kGy dose using a $^{60}$Co gamma source. This dose is higher than normally used for induced-TL studies because Semarkona has exceptionally low TL sensitivity (SEARS et al., 1980). The effects of using large doses has been discussed by MATSUNAMI et al. (1992). The TL measurements were made immediately after irradiation by placing the slice on a Leitz 1350 heating stage and heating to 500°C at 0.25°C/sec in a nitrogen atmosphere. The spatial distribution of the induced TL was measured with the readout system of NINAGAWA et al. (1990) attached to the microscope. An image intensifier with a bialkali photocathode was used with a Corning 4-96 band-pass filter, which transmitted 360 nm to 580 nm, to suppress blackbody radiation. The TL recorded on videocassettes as a function of temperature and location on the slice was analyzed using the two-dimensional photon counting method of YAMAMOTO et al. (1987) and NINAGAWA et al. (1990), modified with the "highly parallel array system" of KOHATA (1991). The spatial resolution of obtained TL image was estimated to be ~70 μm (K. NINAGAWA et al., unpubl. data). Using this system, we can distinguish chondrules with different TL intensities and obtain spatial distribution of high TL areas in a chondrule. The TL spectra were also recorded as a function of temperature and wavelength, substituting a spectroscope for the microscope (NINAGAWA et al., 1986).

For CL observations of the samples, we used a Nuclide Corporation 'Luminoscope' attached to an optical microscope with an electron beam of 14 ± 1 keV and 7 ± 1 μA, a 35 mm Camera and Kodak VR400 film, and exposures of 1.5–3.5 min (SEARS et al., 1991).

After TL measurement, the sections were examined by scanning electron microscopy. Comparison of the TL and BSE images enabled the identification of TL sources. Quantitative analysis of the relevant phases was then performed with an automated JEOL JCXA-733 electron microprobe operating at 15 kV accelerating voltage and 12 nA probe current. The data were corrected using the ZAF method. In this study, electron microprobe analyses of olivine and mesostasis in the slice of Semarkona generally totalled 98.5–100.5 wt% for olivine and 98.0–99.7 wt% for mesostasis, respectively.

## RESULTS

### Induced TL Image, CL Image and Glow Curve

The backscattered electron (BSE) and induced TL images of a chondrule in Semarkona are shown in Fig. 1a and b. The chondrule has high levels of induced TL. The spatial resolution of the TL image (~70 μm) cannot provide detailed distribution of areas with high induced TL in this chondrule. This is mainly because the typical size of crystals and mesostasis areas is smaller than the spatial resolution of the TL imaging system. Nevertheless, we can find some marked features of the image. Especially, the induced TL image has an approximately concentric zoning, the outer margins being highest in induced TL.

CL image of the chondrule appears in Fig. 1c. It is clearly shown that this chondrule has both bright red CL from low-Fe phenocrystic olivine and bright yellow CL from chondrule mesostasis. It is noteworthy that the mesostasis also has a nearly concentric zoning, the outer margins being brightest in CL. The zonal structure of bright yellow CL in the mesostasis is almost consistent with the nearly concentric zoning in the induced TL image.

The TL glow curve (curve of light produced against heating temperature) of the chondrule is shown in Fig. 2. The temperature of the maximum TL emission is about 300°C and the half-width is ~180°C. NINAGAWA et al. (1992) have reported glow curves of three chondrules in Semarkona. Their data suggest that in Semarkona, group A1 chondrules tend to have higher TL peak temperatures (= ~240–300°C) than group B1 chondrules (peak temperature ~ 160°C).

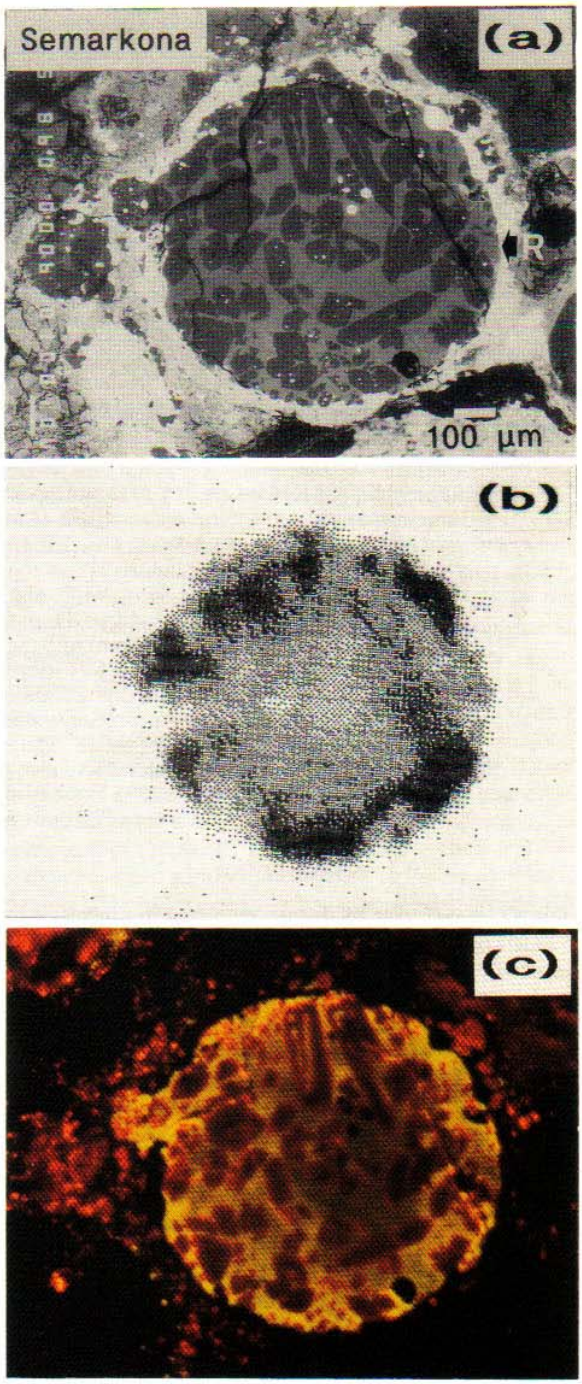


FIG. 1. BSE, induced TL and CL images of a slice sample of the Semarkona (LL3.0) chondrite. (a) BSE image of the sample. White bar 100 μm. "R": an area of the marginal part, where TL intensity is relatively lower than other marginal areas with intense TL (see Fig. 8a).; (b) The induced TL image of the sample in the 40–440°C range. The sample was irradiated by Co-60 gamma-rays and received a dose of 13.2 kGy. The position with high TL intensity is expressed by concentration of black points. The distribution of TL intensity is remarkably heterogeneous and shows an approximately concentric zoning. The marginal part of the chondrule shows TL intensity higher than the central part by a factor of about 6.; (c) CL image of the sample. Images (a), (b), and (c) are to the same scale. Long dimension is 1.4 mm.

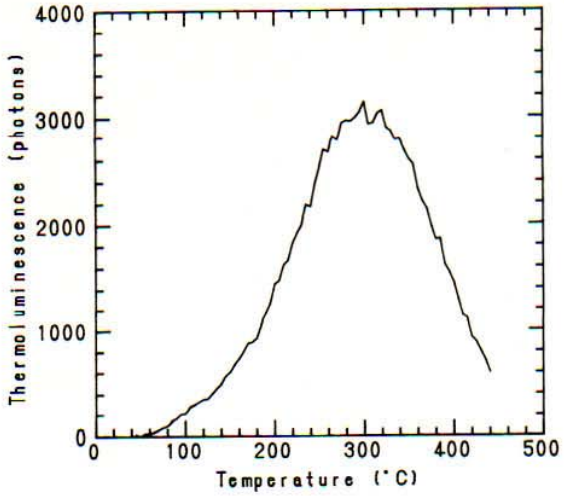


FIG. 2. TL glow curve of a chondrule with high TL in Semarkona. This was obtained by two-dimensional photon counting method (YAMAMOTO et al., 1987) in the 40–440°C range.

## Petrographic Description

This high TL chondrule has an igneous texture consistent with formation by crystallization from a molten droplet (Fig. 1a). It is circular in section, about 800 $\mu$m in diameter, although we can find two small protuberant parts, the uppermost and left-handside parts of the section. They appear to be chondrule-like objects, which have adhered to the surface of chondrule melt during chondrule formation. Since the sizes are less than 100 $\mu$m, they do not seem to have significant influences to the chemical properties of the chondrule. This chondrule contains abundant olivine crystals and spherules of metallic Fe-Ni in the mesostasis. The olivines are euhedral and slightly skeletal with well-formed crystal faces in contact with the mesostasis. The olivine grain size is 10–300 $\mu$m with a mean of 46 ± 33 $\mu$m (=1$\sigma$), a little larger than the values previously reported in type IA chondrules (15–40 $\mu$m, SCOTT and TAYLOR, 1983). Low-Ca pyroxene phenocrysts are absent, but rounded grains of metallic Fe-Ni are distributed throughout the olivines and mesostasis of the chondrule. Modal analysis using point counting method in vol% is as follows: 54 olivine, 45 mesostasis, and 1 metallic Fe-Ni.

Average core and rim composition of the olivine phenocrysts in the chondrule are given in Table 1. This chondrule is characterized by very FeO-poor olivine ($Fa_{0.3-0.5}$), somewhat lower than the values of $Fa_{0.5-2.4}$ reported for fifteen Semarkona type-IA chondrules by JONES and SCOTT (1989). However, like the earlier studies, the olivines in this chondrule are not zoned significantly. The abundances of the minor elements (CaO, $Al_2O_3$, $TiO_2$, $Cr_2O_3$, and MnO) are comparable with those of the most FeO-poor olivines in the study of JONES and SCOTT (1989).

The mesostasis appears glassy to partly microcrystalline on the scale of the BSE image, with most of the microcrystalline areas being in the outer region of the chondrule. Microprobe analyses of mesostasis compositions were obtained using 5–10 $\mu$m electron beams in order to reduce alkali loss from the mesostasis. The mesostasis is generally rich in $SiO_2$, $Al_2O_3$, and CaO and depleted in FeO, $Na_2O$, and $K_2O$ (Table 1), being on average 52.5 wt% normative anorthite. Like the induced TL, the mesostasis is compositionally zoned in Na and Mn. From the analyses and modal compositions, we can estimate the chemical composition of the bulk silicate portion of the chondrule (Table 1). The data display a pattern of decreasing abundance with increasing volatility (Fig. 3) and closely resemble the INAA data obtained by LU et al. (1990) for other group A1 chondrules.

TABLE 1. Chemical compositions of olivine phenocrysts, mesostasis, Ca-rich pyroxene, and bulk silicate portion of a group A1 chondrule with high TL in the Semarkona (LL3.0) chondrite, obtained by EPMA

| | Olivine | | | | | |
|---|---|---|---|---|---|---|
| N* | (core) 10 | (rim) | Ca-rich px in mesostasis 5 | Mesostasis 26 | Al-rich part in a marginal area 2 | Bulk silicate portion |
| $SiO_2$ | 42.5 | 42.4 | 51.9 | 52.4 | 53.9 | 47.4 |
| $TiO_2$ | .06 | .06 | 1.30 | .93 | .12 | .45 |
| $Al_2O_3$ | .25 | .15 | 12.0 | 20.5 | 25.6 | 9.55 |
| $Cr_2O_3$ | .15 | .23 | .67 | .41 | .09 | .29 |
| FeO† | .39 | .48 | .69 | .39 | .35 | .38 |
| MnO | .03 | .04 | .39 | .13 | .04 | .08 |
| MgO | 55.7 | 55.6 | 13.6 | 6.91 | 2.53 | 33.6 |
| CaO | .40 | .36 | 17.7 | 15.9 | 15.4 | 7.74 |
| $Na_2O$ | —‡ | — | .73 | .97 | 1.73 | .42 |
| $K_2O$ | — | — | — | — | .03 | — |
| NiO | — | — | .05 | .05 | .09 | .03 |
| $P_2O_5$ | — | — | — | .13 | .21 | .04 |
| Total | 99.48 | 99.32 | 99.03 | 98.72 | 100.09 | 99.98 |
| Fa | .39 | .47 | | | | |
| En | | | 51.2 | | | |
| Fs | | | 1.5 | | | |
| Wo | | | 47.3 | | | |

* number of averaged analyses
† total as FeO
‡ not detected

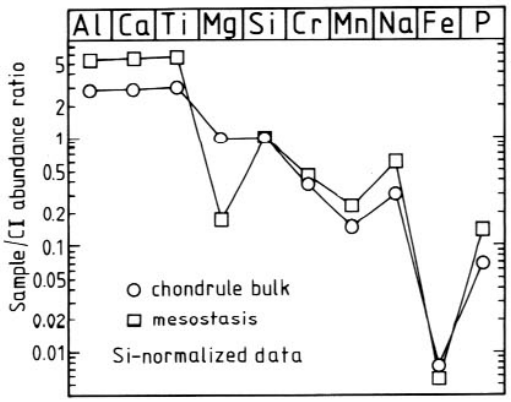


FIG. 3. Elemental abundances in the mesostasis and bulk silicate portion of a chondrule with intense TL in Semarkona. Data are Si-normalized values to CI (ANDERS and EBIHARA, 1982). Open circle: bulk silicate portion; Open square: mesostasis.

Tiny crystals of Ca-rich pyroxene in the mesostasis were also observed and were coarse enough (~5 $\mu$m) to obtain electron microprobe data (Table 1).

### TL and Compositional Zoning Profiles

Two zoning profiles of mesostasis were measured by traversing the mesostasis from the center to the rim: Series I and Series II. The former, twelve points from No. 1 to No. 12, and the latter, fourteen points from No. 1 to No. 14, were selected to examine the variability of TL and compositional zoning trends in the mesostasis (Fig. 4).

The zoning profiles are shown in Fig. 5. Both series show similar tendencies of variation from core to rim. However,

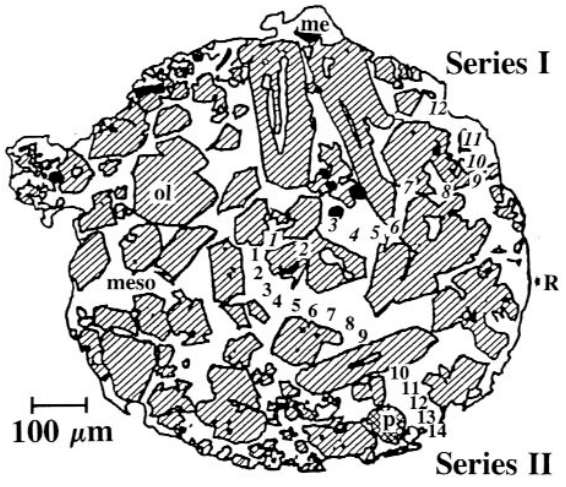


FIG. 4. Sketch of a porphyritic olivine chondrule (group A1) with high TL in Semarkona. Forsterite phenocrysts ($Fa_{0.3-0.5}$) are embedded in Ca,Al-rich mesostasis. The twelve positions for step scan analysis from core (No. 1) to rim (No. 12) (Series I) and the fourteen positions from No. 1 to 14 (Series II) within the mesostasis of the chondrule are also shown in this figure. ol: olivine; meso: mesostasis; me: metallic Fe-Ni; p: pore. Black bar represents 100 $\mu$m. "R": see the captions of Figs. 1a and 8.

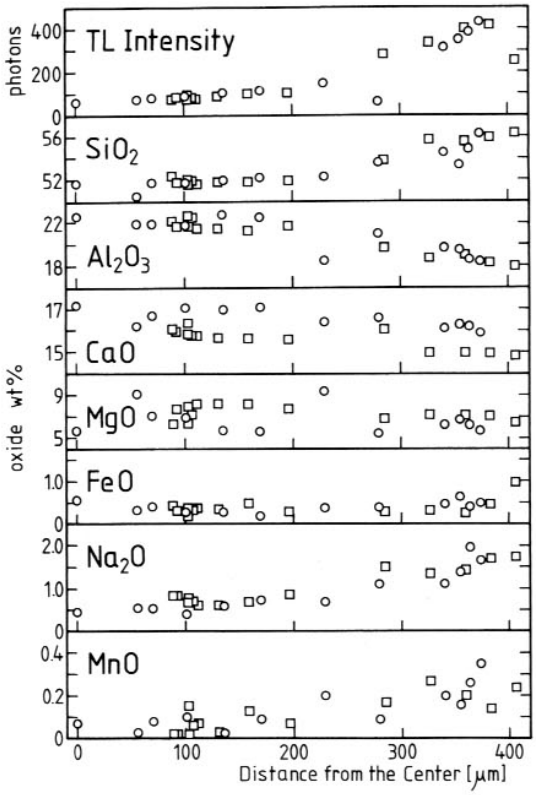


FIG. 5. A diagram showing zoning of chemical compositions and TL intensity within the mesostasis from core to rim of a chondrule with high TL in Semarkona. The local TL intensity was obtained by two-dimensional photon counting method (YAMAMOTO et al., 1987). Both $Na_2O$ and MnO contents and TL intensity increase markedly from core to rim of the chondrule. Open circles: Series I; Open squares: Series II.

we can find systematic differences of CaO and MgO contents in mesostasis. The Series I data have higher CaO and lower MgO contents than the Series II data. The differences can be explained by the local differences of degree of olivine crystallization in the mesostasis. We interpret that the former was affected by a higher degree of olivine crystallization than the latter, because the positions of Series I are relatively near to the surfaces of olivine phenocrysts compared to those of Series II.

The $SiO_2$ content increases monotonically from 52 to 56 wt%, and the $Al_2O_3$ content monotonically decreases from 22 to 18 wt% from the core to the rim of the chondrule (Fig. 5). The CaO content also decreases from 17 to 15 wt%. The content of MgO and FeO show no systematic variation, although their scatter may obscure any trends. $Na_2O$ and MnO increase from core to rim by factors of ~3.6 and ~6, respectively. The TL intensity at each spot was obtained by two-dimensional photon counting over an area of 20 $\mu m^2$ (YAMAMOTO et al., 1987). The induced TL profile is very similar to the variations of $Na_2O$ and MnO contents, monotonically increasing from the center to the margin by a factor of about 6. Decrease of TL intensity on the right end of the diagram (No. 14 of Series II) is considered to be because the

obtained TL intensity is affected by the presence of the edge of the chondrule. The concentric TL pattern is related to the compositional zoning of $Na_2O$ and MnO contents within the chondrule mesostasis. Especially, Mn zoning is important, because it increases by the same order of magnitude to TL zoning.

## DISCUSSION

### Refractory Mesostases in Semarkona Chondrules

Cathodoluminescence photographs have shown that Semarkona contains ~35% by number of chondrules with refractory mesostases, which are conspicuous for their bright yellow CL, often accompanied with bright red CL from FeO-poor olivines (e.g., Fig. 1c; DEHART et al., 1992a). They are rare or absent in other type 3 chondrites. In other type 3 chondrites, chondrules show either no CL or their mesostases display the blue CL typical of sodic feldspars. For type < 3.3 ordinary chondrites, TL glow curves (curves of light produced against heating temperature) are broad and characteristically hummocky, and CL images show that this is because there are a great many phosphors producing the TL in these classes (DEHART and SEARS, 1986; GUIMON et al., 1988).

CL provides good means of addressing this type of the zonal structure described here in the mesostases with bright yellow CL. We have now made CL mosaics of four reasonable-sized sections. We have found that chondrules with this type of the zoning are rare in Semarkona.

Over the 200–350°C temperature range, the 370–650 nm TL emission spectrum of the chondrule described here shows a 100 nm-wide band at ~570 nm (Fig. 6). The TL emission spectra of four type 5 ordinary chondrites have a broad band at ~470 nm in the 150–250°C range, which STRAIN et al. (1985) attributed to $Mn^{2+}$ luminescence sites in oligoclase. HUNTLEY et al. (1988) reported that a 570 nm band was characteristic of twelve relatively calcic feldspar samples which they also attributed to $Mn^{2+}$ substituting for $Ca^{2+}$.

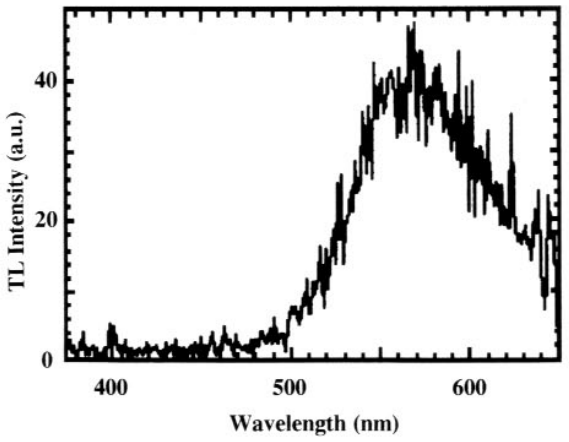


FIG. 6. TL emission spectrum of a group A1 chondrule with high TL in Semarkona in the 370–650 nm range at the temperature interval 200–350°C. The TL emission spectrum was directly measured by a time-resolving spectroscopy system (NINAGAWA et al., 1986). It shows a wide emission band peaked at about 570 nm with a half-width of about 100 nm.

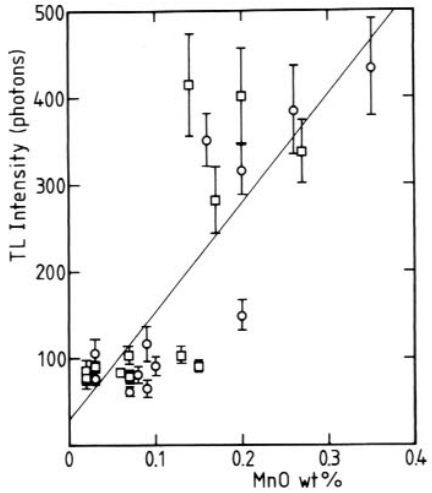


FIG. 7. The relationship between local TL intensity (photons) and the MnO content (wt%) in the mesostasis. The local TL intensity was obtained by a two-dimensional photon counting method (YAMAMOTO et al., 1987). The error bars represent $\pm 1\sigma$, which results mainly from possible errors in determining the positions of step scan analysis on TL image. It shows a positive correlation with the MnO content. A least squares fit of the data gives a linear line almost through the origin of the diagram ($r = 0.82$), strongly suggesting that $Mn^{2+}$ ions are closely related to the intense TL emission of the mesostasis.

In this chondrule, the TL intensity correlates well with the MnO content in the mesostasis (Fig. 7; $r = 0.82$), although we can find somewhat of a scatter of plotted data around the linear regression line. This might also indicate Mn activation, because we can present a simple explanation about this positive correlation. The main factors controlling the local TL intensity in the mesostasis are volume percent of the TL phosphor and the concentration of luminescence sites in the phosphor. As the first approximation, we can assume that the volume percent of the TL phosphor is approximately constant throughout the mesostasis. The increase of the MnO content in the mesostasis would contribute to the increase of the concentration of luminescence sites in the phosphor, unless the latter is intensely affected by crystallization of other phases in the mesostasis. The Mn-TL correlation can be explained by the increase of total $Mn^{2+}$ content in calcic feldspar caused by the increase of the total amount of Mn in the local area. Although the Na content of the mesostasis also correlates positively with induced TL intensity, we suggest that the Mn-TL correlation has more important meanings than the Na-TL correlation. This is partly because of the spectrum indicative of Mn-activation and partly because of the fact that the Mn content increases from core to rim by the same factor as the TL intensity (~6) in the mesostasis.

Recent dynamic crystallization experiments and CL studies of type I chondrule compositions have shown that the phosphor emitting yellow CL in the mesostases of type I chondrules easily formed from melts by the fractionation processes that occur during crystallization (DEHART and LOFGREN, 1991). It is suggested that the phosphor responsible for the yellow CL is calcic plagioclase or calcic pyroxene (SEARS et al., 1991). More recently DEHART et al. (1992b) have identified anorthite and minor high-Ca clinopyroxene crystals in

the mesostases using transmission electron microscopy. These studies indicate that anorthite is the main constituent of the mesostases with bright yellow CL and that it would have easily formed in the chondrule melts by fractional crystallization processes during chondrule formation.

It is also possible that Ca-rich pyroxene could be responsible for the yellow CL, as observed in various terrestrial samples (MARSHALL, 1988). Figure 8a is an enlarged BSE image of a low TL region in the margin of the mesostasis. Several rows of Ca-rich pyroxene are visible, and there is heterogeneous distribution of Al (Fig. 8d), with an enrichment of Al besides rows of Ca-rich pyroxene (~25 wt% $Al_2O_3$). Apparently, crystallization of Ca-rich pyroxene caused Al enrichment in the adjacent mesostasis. Analyses are given in Table 1. Since the Ca-rich pyroxenes contain up to 0.39 wt% MnO, the crystallization has reduced the MnO of the mesostasis (0.04 wt% MnO, Table 1) and caused a resultant decrease in $Mn^{2+}$ content in Ca-rich plagioclase and TL intensity. If type IA chondrules in Semarkona crystallized at cooling rates of the order of 1000°C/h (JONES and SCOTT, 1989), Ca-rich pyroxene could not crystallize throughout the mesostasis and the mesostasis remained largely glassy. This may have helped to increase the MnO content in Ca-rich plagioclase and thereby the TL intensity in the mesostasis. The scatter of data in the Mn-TL correlation diagram (Fig. 7) might suggest that the effect of Ca-rich pyroxene crystallization is somewhat superimposed on variations in induced TL resulting from bulk chemistry of the mesostasis. In short, detailed petrographic studies suggest that Ca-rich pyroxene is not the principal source of the strange TL in this chondrule. Alternatively, we suspect that the major TL phosphor in the mesostasis of group A1 chondrules in Semarkona is calcic feldspar.

## Origin of the Induced TL and Compositional Zoning in the Mesostasis

Possible factors that could affect a chondrule are the chemical composition of the precursor materials, melting, crystallization and interaction with the nebula during and immediately subsequent to chondrule formation, and metamorphic recrystallization or aqueous alteration after accretion (JONES and SCOTT, 1989). Thus, there are six possible mechanisms for producing the mesostasis zoning: (1) differences in the degree of olivine crystallization during cooling of the chondrule; (2) diffusional transport of ions due to a steep temperature gradient within chondrule melt (the Soret effect); (3) infiltration of Na and Mn from the outside of the chondrule during aqueous alteration after accretion; (4) concentric heterogeneities in the composition of the precursor materials; (5) recondensation of volatile elements into the chondrule; and (6) reduction of precursor dust aggregate.

### *Fractional crystallization*

The compositional profiles of the mesostasis are not consistent with possibility (1). If the degree of fractional crystallization of olivine was different in the inner and outer parts of the droplet, and homogenization of the melt due to diffusion was not effective, olivine crystallization would have caused nonuniform distribution of elements in the residual liquid. If the amount of olivine crystallized in the outer part of the chondrule was larger than that in the center, enrichments of Si, Al, Ca, Na, and Mn in the liquid phase would have been observed at the outer part of the chondrule. Although the profiles of $SiO_2$, MnO, and $Na_2O$ contents in the mesostasis are consistent with the above mechanism, the $Al_2O_3$ and CaO decrease monotonically from the center to the rim, suggesting that we can rule out possibility (1). We also think that the textural and compositional uniformity of the olivines argues against fractional crystallization being a factor in the compositional and TL profiles of the mesostasis.

### *Soret effect*

Experimental studies have shown that steep temperature gradients in charges of a lunar highlands magmatic liquid cause migration of elements, with, for example, $SiO_2$ moving to the hotter parts of the charges (WALKER et al., 1981). $Na_2O$ and $K_2O$ also migrate to the hot end of the charge. As the mesostasis of the chondrule described here is depleted in alkalis ((Na + K)/Al = 0.07), Al is expected to fractionate to the center of the droplet (cf. Fig. 3 of WALKER et al., 1981). Compositional profiles of Si, Al, and Na seem to be consistent with Soret separation. However, in the experiments of WALKER et al. (1981), Fe, Mn, Mg, and Ca fractionated to the cold end of the charge. The distribution of Ca is consistent, whereas in the present case Fe and Mg are unzoned and Mn increases to the margins. We conclude that possibility (2) does not provide a reasonable explanation for the TL and compositional zoning of the mesostasis.

### *Element transport into the chondrule during aqueous alteration*

The Semarkona chondrite has clearly suffered small amounts of aqueous alteration since calcite and smectite are present (NAGAHARA, 1984; MATSUNAMI, 1984; HUTCHISON et al., 1987). During aqueous alteration Na might have been transported to the chondrule and infiltrated into the interior. However, as mentioned above, the chondrule shows no textural evidence for aqueous alteration, and we did not detect smectite in the mesostasis using the SEM or microprobe. In fact, the bright yellow CL is also inconsistent with smectite in the outer regions of the chondrule (SEARS et al., 1991). Also, we doubt that the compositional profiles are consistent with aqueous alteration, since Ca would have been readily leached to form Ca carbonates in the matrix (NAGAHARA, 1984; MATSUNAMI, 1984; HUTCHISON et al., 1987), and the observed profiles for Si and Al would not be expected. It is therefore unlikely that compositional zoning is due to the infiltration of volatiles during aqueous alteration.

### *Zoned precursor*

GROSSMAN and WASSON (1983) suggested that Semarkona chondrules were a mixture of refractory, Ca, Al, and Mg-rich material and nonrefractory, Si, Fe, and volatile-rich material. Thermodynamically, Mn would condense at ~1200 K as $Mn_2SiO_4$ and $MnSiO_3$ solid solutions in olivine and orthopyroxene, respectively (WAI and WASSON, 1977). In this context, it is interesting to note that KLÖCK et al. (1989) have discovered submicron olivines and low-Ca pyroxenes

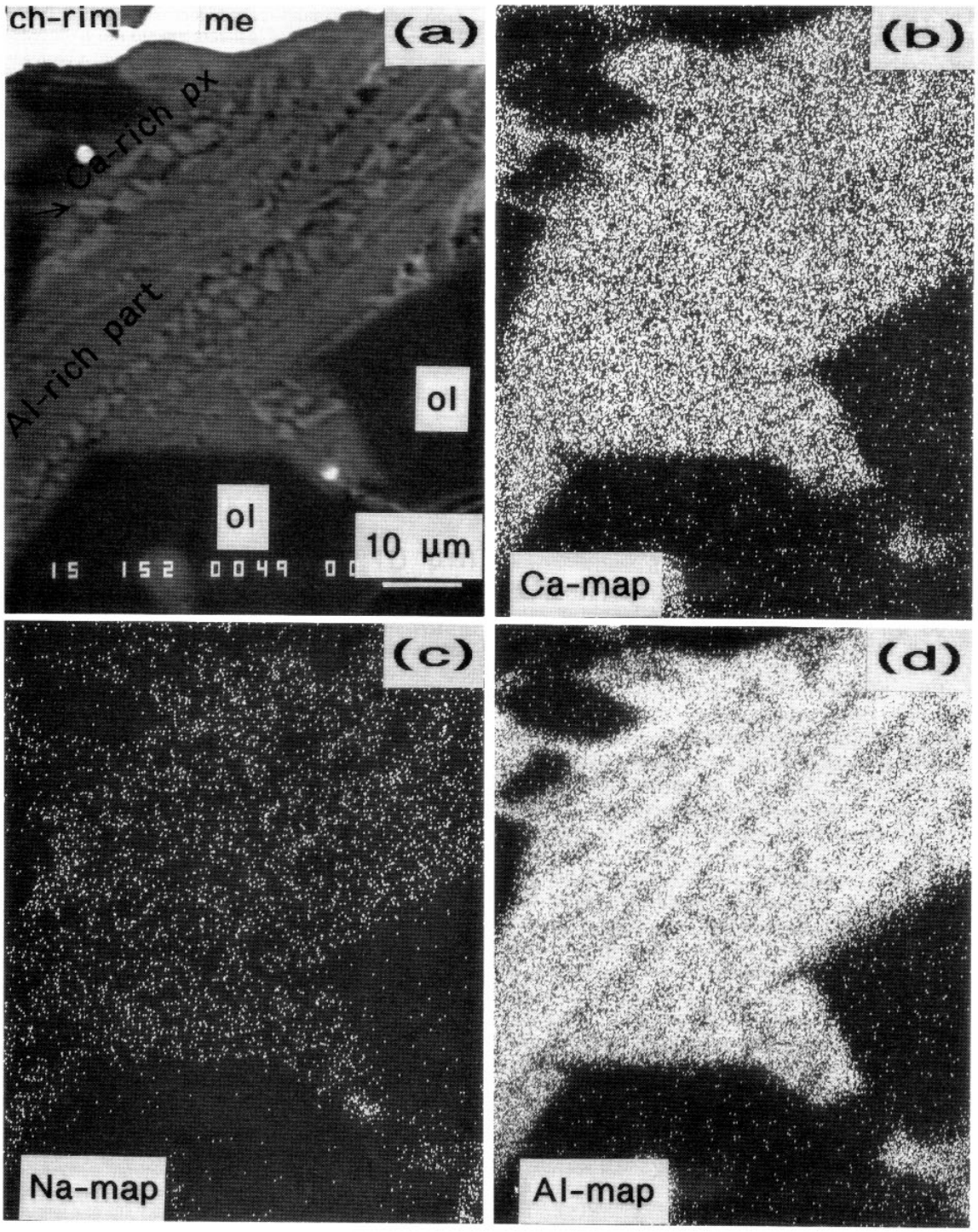


FIG. 8. Distributions of Ca, Na, and Al in a marginal area of the mesostasis with TL intensity relatively lower than other marginal areas. (a) BSE image of the marginal area denoted as "R" in Figs. 1a and 4. Several rows of Ca-rich pyroxene crystals are observed; (b, c, d) X-ray maps showing the distributions of Ca, Na, and Al in the same area. (b) Ca map. Calcium in this area is almost uniformly distributed and is considered to have been mostly preserved in the original state, indicating that this chondrule would not have been affected by any aqueous alteration; (c) Na map. Sodium is also uniformly distributed; (d) Al map. Heterogeneous distribution of Al is observed in this area and Al is clearly enriched besides rows of Ca-rich pyroxene. This is because crystallization of Ca-rich pyroxene would have caused Al enrichment in the remaining parts of the mesostasis near Ca-rich pyroxene. The crystallization of Ca-rich pyroxene also would have made the Al-enriched parts Mn poor, leading to the decrease of $Mn^{2+}$ content in Ca-rich plagioclase and the resultant decrease of TL intensity of this area in the mesostasis.

with high Mn (up to 5 wt% MnO) and low Fe contents in interplanetary dust particles and Semarkona matrix. The refractory component might therefore have consisted of grains of forsterite, Ca-rich pyroxene, and anorthite, while the nonrefractory component may have consisted of silica, albite, and Fe- and Mn-bearing olivines and pyroxenes (MATSUNAMI et al., 1990). If the components were not thoroughly mixed, but produced a concentrically zoned dust aggregate with the refractory component in the center surrounded by the nonrefractory component, then the melted droplet may have been compositionally zoned in the way observed. Somewhat similar to the aggregates described here are the porphyritic Allende chondrules with coarse-grained rims which consist, in part, of manganiferous olivines and pyroxenes (RUBIN, 1984).

The major uncertainty in this mechanism is whether the compositional profiles of the precursors could have survived chondrule melting and olivine crystallization, without also producing olivine textural and compositional evidence. Moreover, the content of MgO and FeO in the mesostasis does not show any clear correlation with silica and volatiles. This seems to be a serious problem for this model.

*Element transport into the chondrule by recondensation*

Sodium and Mn are moderately volatile elements, having 50% condensation temperatures in a system of solar composition of 900–1200 K (WAI and WASSON, 1977). JONES and SCOTT (1989) explained low Na abundances in type IA Semarkona chondrules as due to either volatile-poor precursors or volatile loss during melting. LU et al. (1990) concluded that Semarkona type I chondrules showed volatile loss during chondrule formation. HEWINS (1991) discussed that low Na concentrations in type I porphyritic olivine chondrules are due to the low abundance of precursor albite and proposed that Na was retained during chondrule formation as the simplest explanation.

We consider an alternative possibility that although Semarkona type IA chondrules experienced loss of volatiles during the melting (LU et al., 1990), some of the evaporated volatiles might recondense to the chondrules during the cooling. Significantly high cooling rates of the chondrules may prevent the volatiles from completely recondensing to the chondrules. If so, it is likely that we can observe evidences for recondensation of volatiles onto the surface and their subsequent diffusion into the interior of the chondrule. The observed mesostasis profiles for Na and Mn are consistent with this mechanism. IKEDA and KIMURA (1985) reported Na zoning of groundmass glass in a chondrule from Allende. Their data clearly show increase of the $Na_2O$ content from 3 to 15 wt% from core to rim. This may be a good example for recondensation of volatiles lost from chondrule melts during or subsequent to chondrule formation.

*Reduction of precursor dust aggregate*

The presence of low-Fe olivines ($Fa_{0.3-0.5}$) and spherules of metallic Fe-Ni in the chondrule suggests that the chondrule would have formed under the reducing condition of nebular gas at high temperatures. From INAA data, LU et al. (1990) have concluded that type I chondrules were formed under more reducing conditions at higher temperatures than type II chondrules. It is possible that interaction with the reducing nebular gas caused reduction of precursor dust aggregate of the chondrule.

Recently MATSUNAMI and EL GORESY (1992) have proposed a theoretical model for reduction of (Mg, Fe) olivine. In the model, reduction of olivine proceeds through transport of cations, vacancies, and oxygen anion along oxygen potential gradient in reduced olivine (forsterite + Fe-metal). Along the Fe-concentration gradient in olivine zone, $Fe^{2+}$ ions diffuse into a reduction front to form Fe metal and vacancies of octahedral sites of olivine. The vacancies are transported from the reduction front to the surface along the oxygen potential gradient. At the surface, they react with forsterite component to form silica (or enstatite). Experimental results of NAGAHARA (1986) support this reaction mechanism. Details of their theoretical treatment for olivine reduction and the applications will be published in separate papers.

At first, we consider the case for reduction of olivine aggregate with the diameter of 1 mm as the simplest approximation. The reduction process causes enrichment of silica at the surface of the aggregate. Using the present model, we can estimate the time scale for reduction of olivine aggregate as a function of Fa mol% of constituent olivine grains. Temperature and $P_{H_2O}/P_{H_2}$ ratio of reducing nebular gas were assumed to be 1500°C and $5 \times 10^{-4}$, respectively. Figure 9 shows calculated time scales for reduction of olivine aggregates. Single crystal olivine with the diameter of 1 mm cannot be reduced within the characteristic time scale for chondrule formation ($t_{CF} \sim 10^{3.5-4.5}$ s). However, olivine aggregates composed of sufficiently small grains (Fa < 10; $d$ = 0.1–1 $\mu$m) are reduced within short time $\sim 10^3$ s ($\ll t_{CF}$). This is because the presence of grain boundaries enhances the diffusivities of various ionic species in olivine aggregates by a

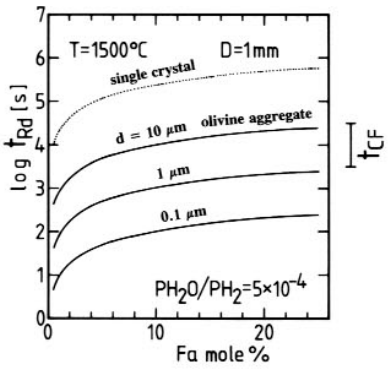


FIG. 9. Time scales for reduction of olivine aggregates with the diameter ($D$) of 1 mm, which are composed of micron-sized olivine with diameter ($d$) of 10 $\mu$m, 1 $\mu$m, and 0.1 $\mu$m, as a function of Fa mol%. Temperature during reduction was assumed to be 1500°C under the condition of $P_{H_2O}/P_{H_2} = 5 \times 10^{-4}$. They were estimated using a theoretical model for reduction of (Mg,Fe) olivine (MATSUNAMI and EL GORESY, 1992). The time scale for reduction of olivine single crystal with the diameter of 1 mm is also plotted. The characteristic time scale for chondrule formation ($t_{CF} \sim 10^{3.5-4.5}$ s), which is imposed by dynamic crystallization experiments of chondrule melts (HEWINS and RADOMSKY, 1990), is shown on the right side of the diagram. Aggregates composed of olivine grains with the diameters of 0.1–1 $\mu$m are reduced within a short time $\sim 10^3$ s ($\ll t_{CF}$).

few orders of magnitude relative to the case for reduction of olivine single crystal. The effect was evaluated using a formula for effective diffusivity in polycrystalline aggregate by STOCKER and ASHBY (1973). Precursor dust aggregate of the chondrule would have contained calcic plagioclase and Ca-rich pyroxene grains as well as Fe-bearing olivine. The presence of these phases causes the aggregate to be partially melted during the temperature rise of chondrule formation. Partial melting of precursor dust aggregate is favorable for the reduction within short time because it also promotes rapid transport of cations and oxygen anions during reduction. The profiles of Al and Ca in the mesostasis reflect simple mass balance through the enrichment of silica at the marginal parts during reduction.

SCOTT and TAYLOR (1983) observed the silica enrichment at the margins of type I chondrules and suggested that it was because of fractional crystallization of olivine. As already discussed, fractional crystallization of olivine cannot explain the compositional zoning of the mesostasis, while the reduction of precursor dust aggregate causes silica enrichment at the surface. We suggest that the reducing conditions would have prevailed during the formation of group A1 chondrules (LU et al., 1990). It probably promoted evaporation of Na and Mn from the chondrule melt. We conclude that both reduction of the precursor and recondensation of volatiles can explain the TL and compositional zoning of the mesostasis consistently.

From these results, the formational process of the chondrule with TL and compositional zoning can be inferred as follows: (1) During the temperature rise of chondrule-forming event, a precursor dust aggregate composed of Fe-bearing olivine, calcic plagioclase, and Ca-rich pyroxene was reduced through interaction with a reducing nebular gas. The reduction process caused increase of silica content at the marginal parts. (2) During melting of the precursor, Na and Mn evaporated from the chondrule melt. (3) During the cooling, forsterite phenocrysts crystallized in the melt. The residual liquid became rich in anorthite component. (4) Subsequently, Na and Mn recondensed onto the surface and diffused into the interior, forming the zoning of Na and Mn. (5) Mn-bearing anorthite then crystallized in the mesostasis. The Mn-zoning caused the difference of Mn contents in anorthite crystallized in the mesostasis, finally leading to the formation of TL and CL zoning.

## CONCLUSIONS

1) A group A1 chondrule in Semarkona with high induced TL has been found to show induced TL and compositional zoning in the mesostasis with induced TL, $SiO_2$, $Na_2O$, and MnO increasing from the center to the rim of the chondrule. The TL intensity is approximately proportional to the MnO content of the mesostasis, and the spectrum of the TL indicates $Mn^{2+}$ activation in Ca-rich plagioclase which crystallized in the mesostasis.
2) The zoning may reflect both reduction of precursor dust aggregate and recondensation of volatile elements onto the surface of the chondrule during or subsequent to chondrule formation. Reducing conditions that prevailed during the formation of a group A1 chondrule with high TL caused both reduction of precursor dust aggregate and evaporation of Na and Mn during melting. The reduction process produced silica-enrichment at the margins of the chondrule. Sodium and Mn profiles were formed through recondensation of these elements onto the chondrule surface and their subsequent diffusion into the interior, leading to the formation of TL and CL zoning in the mesostasis.

*Acknowledgments*—This work was carried out in part under the Visiting Researcher's Program of the Research Reactor Institute, Kyoto University. The authors would like to thank M. Nakagawa for TL spectra measurements. We are grateful to H. Hasegawa, Y. Ikeda, and A. El Goresy for useful comments. We are also grateful to R. H. Jones, G. E. Lofgren, and R. H. Hewins for helpful reviews.

*Editorial handling:* G. Faure

## REFERENCES

ANDERS E. and EBIHARA M. (1982) Solar-system abundances of the elements. *Geochim. Cosmochim. Acta* **46,** 2363–2380.

DEHART J. M. and LOFGREN G. E. (1991) Dynamic crystallization experiments and cathodoluminescence studies of type I chondrule compositions. *Lunar Planet. Sci. XXII,* 291–292.

DEHART J. and SEARS D. W. G. (1986) Cathodoluminescence of type 3 ordinary chondrites. *Lunar Planet. Sci. XVII,* 160–161.

DEHART J. M., LOFGREN G. E., LU J., BENOIT P. H., and SEARS D. W. G. (1992a) Chemical and physical studies of chondrites: X. Cathodoluminescence and phase composition studies of metamorphism and nebular processes in chondrules of type 3 ordinary chondrites. *Geochim. Cosmochim. Acta* **56,** 3791–3807.

DEHART J. M., KELLER L., PROTHROE W., and LOFGREN G. E. (1992b) TEM and cathodoluminescence spectroscopic studies of type A chondrule mesostases. *Lunar Planet. Sci. XXIII,* 295–296.

GROSSMAN J. N. and WASSON J. T. (1983) Refractory precursor components of Semarkona chondrules and the fractionation of refractory elements among chondrites. *Geochim. Cosmochim. Acta* **47,** 759–771.

GUIMON R. K., SEARS D. W. G., and LOFGREN G. E. (1986) The thermoluminescence sensitivity-metamorphism relationship in ordinary chondrites: Experimental data on the mechanism and implications for terrestrial systems. *Geophys. Res. Lett.* **13,** 969–972.

GUIMON R. K., LOFGREN G. E., and SEARS D. W. (1988) Chemical and physical studies of type 3 chondrites: IX. Thermoluminescence and hydrothermal annealing experiments and their relationship to metamorphism and aqueous alteration in type <3.3 ordinary chondrites. *Geochim. Cosmochim. Acta* **52,** 119–127.

HEWINS R. H. (1991) Retention of sodium during chondrule formation. *Geochim. Cosmochim. Acta* **55,** 935–942.

HEWINS R. H. and RADOMSKY P. M. (1990) Temperature conditions for chondrule formation. *Meteoritics* **25,** 309–318.

HUNTLEY D. J., GODFREY-SMITH D. I., THEWALT M. L. W., and BERGER G. W. (1988) Thermoluminescence spectra of some mineral samples relevant to thermoluminescence dating. *J. Lumines.* **39,** 123–136.

HUTCHISON R, ALEXANDER C. M. O., and BARBER D. J. (1987) The Semarkona meteorite: First recorded occurrence of smectite in an ordinary chondrite, and its implications. *Geochim. Cosmochim. Acta* **51,** 1875–1882.

IKEDA Y. and KIMURA M. (1985) Na-Ca zoning of chondrules in Allende and ALHA77003 carbonaceous chondrites. *Meteoritics* **20,** 670–671.

IMAEDA K. et al. (1985) Spatial distribution readout system of thermoluminescence sheets. *Nucl. Instrum. Methods* **A241,** 567–571.

JONES R. H. and SCOTT E. R. D. (1989) Petrology and thermal history of type IA chondrules in the Semarkona (LL3.0) chondrite. *Proc. 19th Lunar. Planet. Sci. Conf.,* B523–B536.

KLÖCK W., THOMAS K. L., MCKAY D. S., and PALME H. (1989) Unusual olivine and pyroxene composition in interplanetary dust and unequilibrated ordinary chondrites. *Nature* **339,** 126–128.

KOHATA M. (1991) A highly parallel array processor system with floating-point digital signal processors. *Trans. Inform. Processing Soc. Japan* **32,** 1142–1148.

LU, J., SEARS D. W. G., KECK B. D., PRINZ M., GROSSMAN J. N., and CLAYTON R. N. (1990) Semarkona type I chondrules compared with similar chondrules in other classes. *Lunar Planet. Sci. XXI,* 720–721.

MARSHALL D. (1988) *Cathodoluminescence of Geological Materials.* Allen Unwin.

MATSUNAMI S. (1984) The chemical compositions and textures of matrices and chondrule rims of eight unequilibrated ordinary chondrites. *Mem. NIPR Spec. Issue* **35,** 126–148.

MATSUNAMI S. and EL GORESY A. (1992) Constraints to the formation of matrix reduced olivine in Yamato-691 (EH3) chondrite: Implications for the evolution of EH chondrites. *17th Symp. Antarctic Meteorites,* 46–49. NIPR.

MATSUNAMI S., NISHIMURA H., and TAKESHI H. (1990) Compositional heterogeneity of fine-grained rims in the Semarkona (LL3) chondrite. *Proc. NIPR Symp. Antarctic Meteorites* **3,** 181–193.

MATSUNAMI S., NINAGAWA K., KUBO H., FUJIMURA S., YAMAMOTO I., WADA T., and NISHIMURA H. (1992) Silica phase as a thermoluminescence phosphor in ALH-77214 (L3.4) chondrite. *Proc. NIPR Symp. Antarctic Meteorites* **5,** 270–280.

NAGAHARA H. (1984) Matrices of type 3 ordinary chondrites—primitive nebular records. *Geochim. Cosmochim. Acta* **48,** 2581–2596.

NAGAHARA H. (1986) Reduction kinetics of olivine and oxygen fugacity environment during chondrule formation. *Lunar Planet. Sci. XVII,* 595–596.

NINAGAWA K., NAKAMURA M., IMAEDA K., TAKAHASHI, N. TOMIYAMA T., YAMAMOTO I., TAKANO Y., YAMASHITA N., YAMASHITA Y., and WADA T. (1986) Time-resolving spectroscopy system. *Bull. Okayama Univ. Sci.* **21A,** 49–54.

NINAGAWA K., YAMAMOTO I., WADA T., MATSUNAMI S., and NISHIMURA H. (1990) Thermoluminescence study of ordinary chondrites by TL spatial distribution readout system. *Proc. NIPR Symp. Antarctic Meteorites* **3,** 244–253.

NINAGAWA K., KUBO H., FUJIMURA S., YAMAMOTO I., WADA T., MATSUNAMI S., and NISHIMURA H. (1991) Thermoluminescence characteristics and chemical compositions of mesostases in ordinary chondrites. *Proc. NIPR Symp. Antarctic Meteorites* **4,** 344–351.

NINAGAWA K., NISHIMURA S., KUBONO N., YAMAMOTO I., KOHATA M., WADA T., YAMASHITA Y., LU J., SEARS D. W. G., MATSUNAMI S., and NISHIMURA H. (1992) Thermoluminescence of chondrules in primitive ordinary chondrites, Semarkona and Bishunpur. *Proc. NIPR Symp. Antarctic Meteorites* **5,** 281–289.

RUBIN A. E. (1984) Manganiferous orthopyroxene and olivine in the Allende meteorite. *Amer. Mineral.* **69,** 880–888.

SCOTT E. R. D. (1984) Classification, metamorphism and brecciation of type 3 chondrites from Antarctica. *Smithsonian Contrib. Earth Sci.* **26,** 73–94.

SCOTT E. R. D. and TAYLOR G. J. (1983) Chondrules and other components in C, O, and E chondrites: Similarities in their properties and origins. *Proc. 14th Lunar Planet. Sci. Conf., Part 1; J. Geophys. Res.* **88**(Suppl.), B275–B286.

SEARS D. W. G. (1988) Thermoluminescence of meteorites: Shedding light on the cosmos. *Nucl. Tracks Radiat. Meas.* **14,** 5–17.

SEARS D. W., GROSSMAN J. N., MELCHER C. L., ROSS L. M., and MILLS A. A. (1980) Measuring metamorphic history of unequilibrated ordinary chondrites. *Nature* **287,** 791–795.

SEARS D. W., GROSSMAN J. N., and MELCHER C. L. (1982) Chemical and physical studies of type 3 chondrites-I: Metamorphism related studies of Antarctic and other type 3 ordinary chondrites. *Geochim. Cosmochim. Acta* **46,** 2471–2481.

SEARS D. W. G., SPARKS M. H., and RUBIN A. E. (1984) Chemical and physical studies of type 3 chondrites-III. Chondrules from the Dhajala H3.8 chondrite. *Geochim. Cosmochim. Acta* **48,** 1189–1200.

SEARS D. W. G., DEHART J. M., HASAN F. A., and LOFGREN G. E. (1989) Induced thermoluminescence and cathodoluminescence studies in meteorites: Relevance to structure and active sites in Feldspar. In *Spectroscopic Characterization of Minerals and Their Surfaces* (ed. L. M. COYNE et al.); *ACS Symp. Ser. 415,* 199–222. Amer. Chem. Soc.

SEARS D. W. G., HASAN F. A., BATCHELOR J. D., and LU J. (1990) Chemical and physical studies of type 3 chondrites-XI: Metamorphism, pairing and brecciation of type 3 ordinary chondrites. *Proc. 21th Lunar Planet. Sci. Conf.,* 493–512.

SEARS D. W. G., BATCHELOR J. D., LU J., and KECK B. D. (1991) Metamorphism of CO and CO-like chondrites and comparisons with type 3 ordinary chondrites. *Proc. NIPR Symp. Antarctic Meteorites* **4,** 319–343.

SEARS D. W. G., LU J., BENOIT P. H., DEHART J. M., and LOFGREN G. E. (1992) A compositional classification scheme for meteoritic chondrules. *Nature* **357,** 207–210.

STEELE I. M. (1986) Compositions and textures of relic forsterite in carbonaceous and unequilibrated ordinary chondrites. *Geochim. Cosmochim. Acta* **50,** 1379–1395.

STOCKER R. L. and ASHBY M. F. (1973) On the rheology of the upper mantle. *Rev. Geophys. Space Phys.* **11,** 391–426.

STRAIN J. A., TOWNSEND P. D., JASSEMNEJAD B., and MCKEEVER S. W. S. (1985) Emission spectra of meteorites during thermoluminescence. *Earth Planet. Sci. Lett.* **77,** 14–19.

WAI C. M. and WASSON J. T. (1977) Nebular condensation of moderately volatile elements and their abundances in ordinary chondrites. *Earth Planet. Sci. Lett.* **36,** 1–13.

WALKER D., LESHER C. E., and HAYS J. F. (1981) Soret separation of lunar liquid. *Proc. 12th Lunar Planet. Sci. Conf.,* 991–999.

WALTON A. J. and DEBENHAM N. C. (1980) Spatial distribution studies of thermoluminescence using a high-gain image intensifier. *Nature* **284,** 42–44.

YAMAMOTO I., IMAEDA K., TAKAHASHI N., NINAGAWA K., TOMIYAMA T., WADA T., and YAMASHITA Y. (1987) Spatial distribution readout system of thermoluminescence sheets II. *Nucl. Instrum. Methods* **A256,** 567–575.